

## Material recognition with a $^{252}\text{Cf}$ source

*Daniela Fabris<sup>a</sup>, Xin Hao<sup>a</sup>, Marcello Lunardon<sup>a</sup>, Sandra Moretto<sup>a</sup>, Giancarlo Nebbia<sup>a</sup>,  
Silvia Pesente<sup>a</sup>, Luca Stevanato<sup>a</sup>, Giuseppe Viesti<sup>a</sup>, Laszlo Sajo-Bohus<sup>b</sup>*

<sup>(a)</sup>INFN and Dipartimento di Fisica, Università di Padova, Via Marzolo 8,  
Padova I-35131, Italy

<sup>(b)</sup>Laboratorio de Fisica Nuclear, Universidad Simon Bolivar, Apartado 89000,  
Caracas 1080A, Venezuela

### Abstract

Material recognition is studied by measuring simultaneously the transmission of neutron and gamma rays produced by a time-tagged  $^{252}\text{Cf}$  source. Light elements (C,N,O) are identified by using the measured transmission versus neutron time of flight. The yield of the transmitted gamma ray as a function of energy provides high precision identification of the atomic number of the sample up to  $Z=83$ . A tomography system, currently under construction, is described.

## 1 Introduction

Non-destructive analysis (NDA) of materials is a well known technique applied in several fields. Material recognition with X-rays [1] is based on the atomic number dependence of the relevant photon absorption coefficients: it is a well established method at low photon energy, while it becomes critical for increasing photon energy, as required in order to increase the penetration of radiation to inspect thick objects [2].

When photon irradiation is unable to disentangle the problem of inspections, the use of neutrons as probing radiation has been often proposed in the past. To this end sophisticated techniques have been developed in order to enhance material recognition, especially for low-atomic-number materials, in an effort to optimize the detection of explosives and drugs in custom operations [3-8].

In this paper we demonstrate the possibility of enhancing the material recognition respect to what obtained previously by using simply the ratio of energy integrated neutron and gamma-ray transmission measurements [7]. This is obtained exploiting the information available from energy dependent transmission measurements allowed by the wide energy spectrum characteristic of a fission source such as  $^{252}\text{Cf}$ .

## 2 Experimental Details

The experimental set-up used in our early measurements consists of a  $10^6$  fissions/s  $^{252}\text{Cf}$  source, tagged requiring the coincidence between two 2" thick 4" diameter NE213 liquid scintillator cells mounted face to face around the source. A full description of the experimental set-up is in ref.9. The tagged radiation is first collimated by a 44 cm long lead-polyethylene collimator and then hits the sample. A third 2" x 4" NE213 liquid scintillator cell is placed at a distance of about 160 cm from the tagged  $^{252}\text{Cf}$  source to detect transmitted neutrons and gamma rays. The low energy threshold of the neutron detector was measured to be about 100 keVee.

In the experiment with fission gamma rays, the NE213 cell was replaced by a 3" thick 3" diameter NaI(Tl) equipped with an anti-coincidence shield, to improve the full-energy response of the detector.

### 3 Experimental Results

#### 3.1 Exploring the neutron/gamma transmission measurements.

As reported in previous work [4,7], material recognition can be obtained from the ratio  $R$  of the absorption coefficients for neutrons  $\mu_n$ , and gamma rays  $\mu_\gamma$ . The latter being the logarithmic ratio of the measured transmission factors for neutrons ( $I_n/I_{n,0}$ ) and gamma rays ( $I_\gamma/I_{\gamma,0}$ ) respectively:

$$R = \mu_n / \mu_\gamma = \ln(I_n/I_{n,0}) / \ln(I_\gamma/I_{\gamma,0})$$

where  $I_n$  and  $I_\gamma$  ( $I_{n,0}$  and  $I_{\gamma,0}$ ) are the measured yields with (without) the sample for neutrons and gamma rays. The ratio  $R$  characterizes a given material and does not depend on the thickness of the sample.

The dependence of the  $R$  value on the material atomic number has been explored in ref.9, employing a large number of elementary samples, ranging from boron to bismuth. The experimental values of  $R$  obtained with the  $^{252}\text{Cf}$  source are reported in Fig. 1. The variation of  $R$  across the atomic number of the samples investigated is equivalent to that determined by the CSIRO group using mono-energetic 14 MeV neutrons and a  $^{60}\text{Co}$  source [7].

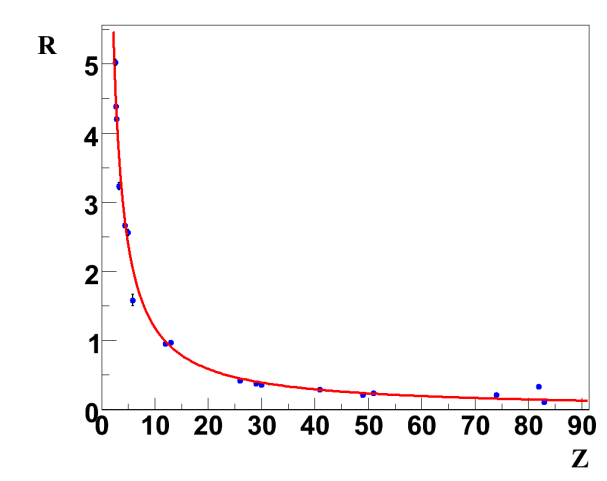


Fig.1.  $R$  values measured with the tagged  $^{252}\text{Cf}$  source. The line refers to the average calibration line.

Looking globally at the measured  $R$  values in Fig.1, it is clear that the data exhibit a rather nice monotonic behaviour with much larger incremental ratio for light samples ( $5 < Z < 13$ ) respect to the heavier ones. The  $Z$  resolving power achievable with this method is a function of the statistical accuracy in the measure of  $R$ . As an example, an accuracy of 5% on  $R$  should correspond to a resolving power  $\delta Z \sim 0.22$  for the lightest samples ( $5 < Z < 13$ ), whereas the same statistical accuracy yields  $\delta Z \sim 9.2$  for heavy samples ( $Z > 26$ ).

#### 3.2 Low $Z$ material: neutron time-of-flight characterization

It is well known that low  $Z$  elements as C,N,O, that are the basic constituents of organic compounds, exhibit strong resonances in the neutron cross section. Such resonances generate absorption dips in the neutron spectrum emerging from the samples, when the transmission is measured by using a white neutron source. Consequently, the analysis of the transmission as a function of neutron energy can be used to identify the light nuclei in an organic sample [3]. Fission sources offer the possibility to look for fast neutron resonances in the range  $E_n=0.2-5$  MeV. This range is limited at low energy by the threshold of the neutron detector and on the high energy side by the relatively low yield of energetic neutrons. Moreover, the time-of-flight resolution of the detection system sets additional constraints on

the detectability of narrow resonances. Nevertheless C,N,O nuclei show a number of bump-like structures in the total cross section that can be used as signatures to identify a particular nucleus.

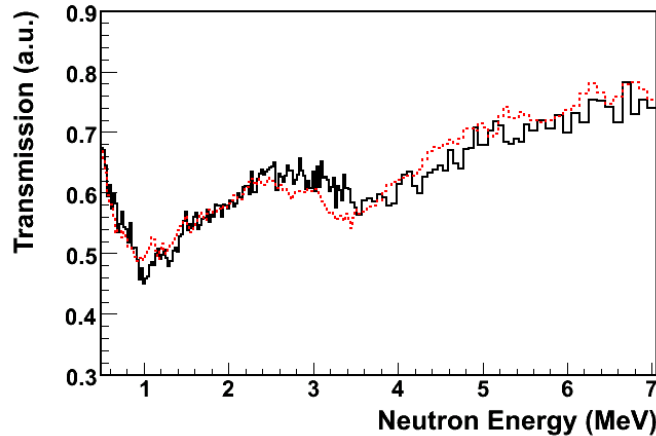


Fig.2 Experimental transmission versus neutron energy spectrum for a paper sample (black). The dotted line is obtained by a least square fit using the weighted sum of elemental C and H<sub>2</sub>O spectra.

As discussed in details in ref.9, it is possible to determine clear identification features in the experimental transmission spectra of C,N,O nuclei. Information about the density of nuclei inside a given complex sample can be thus obtained by fitting the experimental spectrum with a library of elemental spectra. As an example we report in Fig.2 the transmission spectrum of a paper sample which has been fitted using a weighted sum of the elemental C (graphite) and H<sub>2</sub>O spectra. The best-fit corresponds to a C/H<sub>2</sub>O ratio of about 1, in agreement with the expected value for such material. Consequently, we can take this as a demonstration of the possibility to use the neutron time-of-flight measurement to derive the chemical composition of an organic sample.

### 3.3 Gamma ray transmission measurements

In order to improve the material recognition for  $Z > 26$  samples, specific tests have been performed by using gamma ray detector with anti-coincidence shield. We assume in the following that the energy released in the NaI(Tl) is representative of the energy of the detected photon. Since the measured peak-to-total is about 70% at about 1.2 MeV and the peak-to-total is expected to decrease at higher energies, this fact would certainly generate systematic uncertainties in the results reported here. Such uncertainty can be avoided in future work by unfolding the measured photon spectrum with energy-dependent detector response functions.

For a given sample of the element  $Z$  with known thickness  $t$ , we measure the transmitted spectrum  $I_{\gamma}^{\text{exp}}(E_{\text{det}}, Z)$ . From the un-attenuated spectrum  $I_{\gamma,0}(E_{\text{det}})$ , measured with the same detector, and using the NIRST database of attenuation coefficients [6], it is possible to predict the transmitted spectrum for a sample of the element  $Z$  and thickness  $t$  by using the well known formula:

$$I_{\gamma}^{\text{calc}}(E_{\text{det}}, Z) = I_{\gamma,0}(E_{\text{det}}) \exp[-\mu(Z,E)t]$$

where the attenuation coefficients at  $E = E_{\text{det}}$  are used without taking into account possible bias due to the detector response function.

Assuming that the element inside the sample is not known, one can compare the measured transmitted spectrum  $I_{\gamma}^{\text{exp}}(E_{\text{det}}, Z)$  with a library of predicted spectra,  $I_{\gamma}^{\text{calc}}(E_{\text{det}}, Z)$ , and then calculate the reduced chi-squared  $\chi^2 / \nu(Z)$  over a defined energy range ( $E_1, E_2$ ) providing the recognition of the sample material. It is worth noting that the difference in the attenuation of photons of a given energy  $E$  for a sample of thickness  $t$  of two neighboring elements  $Z$  and  $Z+1$  depends not only on the change in

the mass attenuation coefficient  $\mu/\rho$  but also on the change on the density of the materials. Consequently, the sensitivity of the method is much larger for the elements for which the density is strongly varying with  $Z$ .

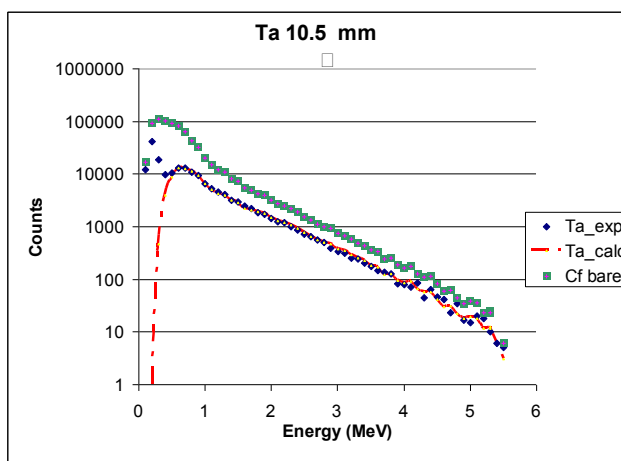


Fig.3 Examples of the gamma ray spectra measured in this work: direct  $^{252}\text{Cf}$  photons (squares), photons transmitted through a 10.5 mm thick Ta sample (diamonds) and predicted distribution (line). For details see the text.

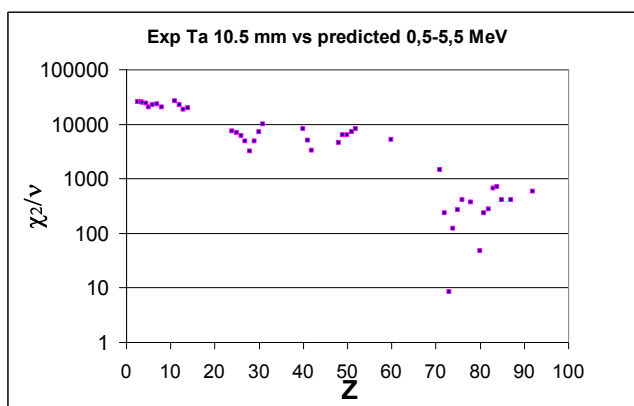


Fig.4  $\chi^2 / \nu$  values as a function of  $Z$  for a 10.5 mm tantalum sample.

As an example of such procedure, measured spectra are reported in Fig.3 and results are shown in Fig.4 in terms of  $\chi^2 / \nu$  values as a function of  $Z$  for a 10.5 mm tantalum sample . A strong minimum appears in the distribution in Fig.4 around  $Z=73$ , from which the first and second moment of the distribution can be evaluated, yielding the most probable atomic number  $\langle Z \rangle$  and the associated uncertainty  $\Delta Z$ .

This procedure has been applied for a quite large number of elementary samples. Results are reported in Fig. 5 in term of measured  $\langle Z \rangle$  versus the sample  $Z$ , showing a very good linearity in material recognition. Moreover, the uncertainty  $\Delta Z$  around the reconstructed most probable value is lower than 3  $Z$  units. Results obtained so far with fission gamma rays are fully presented in ref.11.

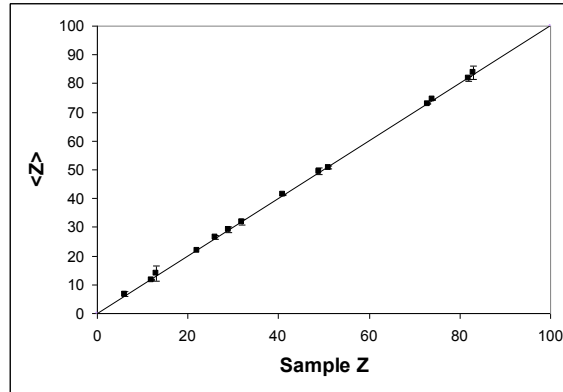


Fig.5 Measured  $\langle Z \rangle$  versus the sample Z. For details see the text.

#### 4. The new tomography system

Following the results presented in previous sections, a new tomography system based on the use of time tagged fission sources has been designed and is now under test. The system, shown in Fig.6, includes both a neutron detector array and the NaI(Tl) detector with anti-coincidence shield used previously. The system will be controlled by using the LabView software for positioning the sample and controlling the data taking for each view. A CAEN VME based DAQ system will be used. Data sorting and data analysis is performed by using the ROOT package.

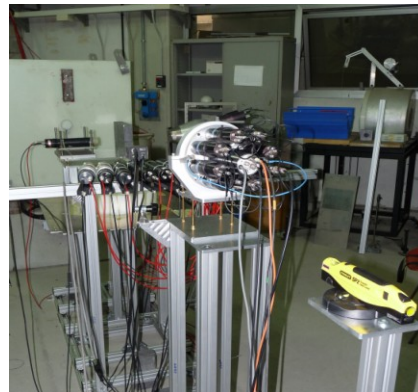


Fig. 6 The new system under test.

The neutron part is based on the use of new scintillation detectors made by 2'' x 2'' right cylinder of EJ228 fast plastics scintillator coupled, by using EJ 560 silicon rubber interface, to a PHOTONIS XP2020 photomultiplier. Such detectors have been selected to improve substantially the time resolution in the time of flight measurement respect to the previous set-up.

Typical time resolutions are reported in Fig. 7, as measured in a  $^{60}\text{Co}$   $\gamma$ - $\gamma$  coincidence run with two of the above detectors, as a function of the low energy threshold in the Constant Fraction Time Discriminator.

It is seen that the time resolution is well below the 0.5 ns level for thresholds above 150 keV, to be compared with  $\delta t = 1.5$  ns [FWHM] obtained in our previous work [9]. This improvement in time resolution allows the use of much shorter flight paths respect the 160 cm previously used. We are currently performing tests with about 60 cm flight path using an array of 8 detectors.

The sample rotating platform will be placed at about 20 cm from the source. In such conditions the

size of the pixel at the sample position has a diameter of less than 2 cm. Such geometry would make the entire system relatively compact.

An example of the time of flight spectra taken with this new set-up is shown in Fig. 8.

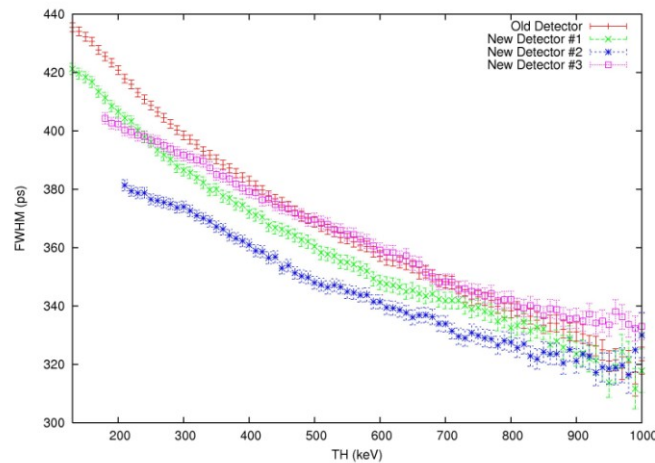


Fig. 7 Time resolution [FWHM] as measured in  $\gamma$ - $\gamma$  coincidences as a function of the CFTD threshold.

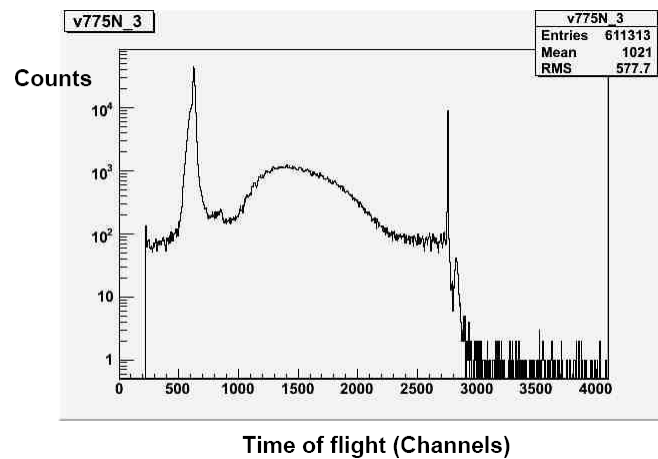


Fig. 8 Time of flight spectrum of the  $^{252}\text{Cf}$  source as measured with the new set-up

## 5. Applications

The neutron/gamma tomography system described in this work has been designed for laboratory applications for which the imaging time would not be a strong requirement. This is due to the low neutron/gamma yield of a time tagged  $^{252}\text{Cf}$  source. However, as discussed in ref. 9, fast inspection systems might be designed in future by using accelerator based neutron/gamma sources using pulsed beams.

Laboratory use of the system is foreseen for all applications in which the bulk material need to be first imaged and analyzed with high resolution. In this respect the system will operate first to reconstruct the 2-D or 3-D material distribution by measuring the R ratio (i.e. the energy integrated neutron-gamma transmission ratio). In a second step it will perform detailed inspections for some key pixels by measuring high statistics neutron time of flight distribution and the photon attenuation.

Tests connected with the latter quantity has been already performed [11]. As an example, we report in Fig. 9 the reconstruction of the Cr/Ni ratio in a typical commercial stainless steel by comparing the experimental transmitted spectrum with the expected one as a function of the Chromium content.

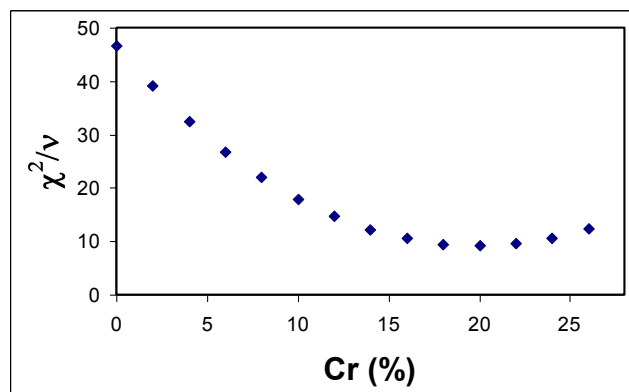


Fig.9 Example of application: determination of the Chromium content in a AC304 stainless steel sample.

## 6. Conclusions

Material recognition by using simultaneous gamma and neutron transmission measurements with the use of  $^{252}\text{Cf}$  has been studied. Specific of the present work is the use of a time tagged source that allows one not only to discriminate neutrons from gamma rays by time of flight information, but also to perform neutron transmission measurements as a function of neutron energy. Gamma ray transmission measurements have been also performed in the energy range 0.1-5.5 MeV.

The material recognition determined by measuring the ratio R of the attenuation factors with gamma rays and neutrons has been extensively studied in ref.9. Results confirm that the ratio R can be used to measure the average atomic number of the investigated material.

In order to improve the material recognition capability for organic samples, the information contained in the neutron transmission versus time of flight has been explored. The measured transmission shows features due to resonances and gross shape of the total neutron cross section clearly identifying light key elements in threat material discrimination (C,N,O). As a direct consequence it is possible to extract the elemental composition of a compound by using a weighted sum of elementary spectra.

On the other side, the measurement of the gamma ray transmission as a function of energy provides, knowing the sample thickness, a very precise material recognition for samples with  $Z > 26$ . This technique has been also applied in testing the composition of commercial stainless steel.

Following the results obtained so far, a new tomography system has been designed and is currently under development.

## Acknowledgements

This project is supported by the “Fondazione Cassa di Risparmio di Padova e Rovigo” under the “2007 Progetti di Eccellenza” scheme.

## References

- [1] H. Vogel, D. Haller, European Journal of Radiology 63 (2007) 242 and references therein.
- [2] S. Ogorodnikov, V. Petrunin, Phys. Rev. ST-AB 5 (2002) 104701
- [3] J. C. Overley et al., Nucl. Instr. Meth. B251 (2006) 470.
- [4] R. J. Rasmussen et al., Nucl. Instr. Meth. B124 (1997) 611.
- [5] J. Rynes et al., Nucl. Instr. Meth. A 422 (1999) 895.
- [6] G. Chen, R. Lanza, R., 2002. IEEE Trans. Nucl. Sci., 49 (2002) 1919.
- [7] J.B. Eberhardt et al, Appl. Radiat. Isot. 63(2005)179
- [8] G. Vourvopoulos and P.C. Womble, P.C., Talanta 54 (2001) 459 and references therein
- [9] G. Viesti et al, Nucl. Instr. Meth. A 593 (2008) 592
- [10] see <http://physics.nist.gov/PhysRefData/XrayMassCoef/cover.html>
- [11] G. Viesti et al, Nucl. Instr. Meth. A606 (2009) 816.